

# Efficient Compression for Remote Sensing: Multispectral Transform and Deep Recurrent Neural Networks for Lossless Hyper-Spectral Image

Dr. D. Anuradha<sup>1</sup>, Gillala Chandra Sekhar<sup>2</sup>, Dr. Annapurna Mishra<sup>3</sup>,  
Dr. Puneet Thapar<sup>4</sup>, Prof. Ts. Dr. Yousef A. Baker El-Ebiary<sup>5</sup>, Maganti Syamala<sup>6</sup>

HOD, Dept. of CSBS, Panimalar Engineering College, Chennai, India<sup>1</sup>

Dept. of Computer Science and Engineering, Institute of Aeronautical Engineering, Dundigal, Hyderabad – 500043, India<sup>2</sup>

Associate Professor, Department of Electronics and Communication Engineering,

Silicon Institute of Technology, Bhubaneswar, India - 751024<sup>3</sup>

Assistant Professor in Computer Science and Engineering Department, Lovely Professional University, Punjab, India<sup>4</sup>

Faculty of Informatics and Computing, UniSZA University, Malaysia<sup>5</sup>

Assistant Professor, Dept. of Computer Science and Engineering, Koneru Lakshmaiah Education Foundation, Vaddeswaram,  
Guntur Dist., Andhra Pradesh - 522302, India<sup>6</sup>

**Abstract**—Remote sensing technologies, which are essential for everything from environmental monitoring to disaster relief, enable large-scale multispectral data collection. In the field of hyper-spectral imaging, where high-dimensional data is required for precise analysis, effective compression techniques are critical for transmission and storage. In the field of hyper-spectral imaging, the development of efficient compression techniques is critical because datasets containing high-dimensional information must be transmitted and stored efficiently without sacrificing analytical precision. The paper presents advanced compression techniques that combine deep Recurrent Neural Networks (RNNs) with multispectral transforms to achieve lossless compression in hyper-spectral imaging. The Discrete Wavelet Transform (DWT) is used to efficiently capture spectral and spatial information by utilizing the properties of multispectral transforms. Simultaneously, deep RNNs are used to model the hyper-spectral data with complex dependencies, allowing for sequential compression. The overall compression efficiency that is increased by the integration of spatial and spectral information allows for reduced storage requirements and improved transmission efficiency. Python software is used to implement the proposed model. When compared to Linear Spectral Mixture Analysis (LSMA) based compression, Spatial Orientation Tree Wavelet (STW)-Wavelet Difference Reduction (WDR), and DPCM, the proposed DWT-RNN-LSTM method has a better PSNR value of 45 dB and a lower MSE of 7.50%. Adaptive compression methods are presented in order to dynamically adapt to various data properties and ensure application in various hyperspectral scenes. Studies on hyper-spectral images of various sizes and resolutions demonstrate the approach's scalability and generalization, as well as the utility and adaptability of the proposed compression framework in a variety of remote sensing scenarios.

**Keywords**—Multi-Spectral transform; lossless compression; hyper-spectral data; deep recurrent neural network; compression algorithms

## I. INTRODUCTION

Spectral imaging uses multiple bands across the electromagnetic spectrum, obtaining data simultaneously from imaging and spectroscopy. Multispectral remote sensors capture data from three to fifteen broad wavelengths, while hyper spectral sensors capture multiple bands. In contrast, several spectral bands spanning a wide wavelength range of 400–2500 nm are concurrently captured by hyper spectral (HS) remote sensors [1]. Spectrophotometry is the foundation of the hyperspectral imaging method. For every spatial area, numerous wavelengths and bands of data from images are collected. With the use of this data, a hyperspectral cube is produced, with the third dimension representing spectral content and the other two representing the location's spatial extent. Materials with varied qualities can be distinguished from one another thanks to the spectral signature, which is the result of particle scattering and molecule absorption [2]. Among the uses for hyperspectral remote sensing include criminal investigation, forecasting weather, agriculture, the food sector, and the medical field [3]. But this richness of information comes at a high memory cost because hyperspectral imagery generates a large amount of data that needs to be stored. These images' extreme richness stems from their high spectral dimensionality, which includes a wide range of spectral channels that capture subtle details about the scene or object under study. Since each pixel contains 16- or 12-bit data, a single HIS dataset might be hundreds of gigabytes (GBs) in size. The range of pixel values can range from a hundreds to millions, and the range of band numbers can be as high as 22 [4]. Compared to RGB and multispectral images, hyperspectral imaging (HSI) has a higher number of bands and a finer spectral resolution [5]. Hyperspectral images can contain dozens or even hundreds of spectral bands, whereas multispectral images usually only have a few. Over the past few decades, hyperspectral imaging has extended beyond traditional ground-based computer vision applications and shown great potential in a variety of fields, including recognizing faces, chemical engineering, farming, biology,

and archaeological research. Its uses include material identification, record or ink aging, pen authentication, visual similarity ink differentiation, and documentation preservation.

With its ability to capture and analyze a wide range of contiguous spectral bands across the electromagnetic spectrum, this advanced imaging technology has become indispensable in a variety of fields, including remote sensing, agriculture, healthcare, and environmental monitoring. Hyperspectral imaging in environmental science allows for the accurate identification and tracking of ecological variables, which helps with well-informed conservation decision-making. It helps with disease detection, crop health assessment, and efficient resource allocation in agriculture. Hyperspectral imaging aids in diagnosis in the medical field by providing in-depth understanding of tissues and biological processes. Additionally, its uses in remote sensing enable businesses to obtain comprehensive data about the surface of the Earth, improving resource management and disaster response. Hyperspectral imaging's versatility and depth of data continue to spur innovation, making it a vital tool for a wide range of academic and professional projects.

One of the main concerns of compression algorithms that aim to reduce data redundancy is the difficulty of analysing large hyperspectral images (HSI) while preserving important information. Data redundancy and compression ratios are crucial in the field of multispectral images, such as Hyperspectral Imaging (HSI). Because redundant information gives compression algorithms plenty of opportunities to take advantage of similarities and patterns, high data redundancy in these images frequently results in elevated compression ratios. Multispectral images exhibit redundancy in four different flavours, each of which has a unique impact on the compression process. Similarities between spectral bands, where adjacent bands may convey similar information, give rise to spectral redundancy. Since neighbouring pixels in multispectral imagery frequently show similarities, spatial redundancy results from redundant information within the same spectral band of images. When thinking about sequential images over time, temporal redundancy is introduced, capturing redundant information across different moments. Lastly, inter-band redundancy adds to the overall redundancy landscape by involving correlations between various spectral bands. It is essential to comprehend and control these different types of redundancy when optimizing compression techniques for multispectral imagery. First, statistical redundancy is analysed through symbol probability, which is commonly done using entropy coding. Second, if pixel information can be partly acquired from nearby pixels and is reduced by transformations, spatial redundancy depends on intraband correlation. Thirdly, spatial decorrelation eliminates spectral redundancy, also known as interband correlation, which results from strong correlations between adjacent bands in hyperspectral images [6].

Finally, visual redundancy uses data quantization for compression based on visual redundancy, which is influenced by the insensitivity of the human eye to high frequencies. Compression methods are divided into two categories: two-dimensional and three-dimensional. They utilize correlations between or within bands [5]. Redundancy in multispectral

images can occur in four ways: spectral redundancy, spatial redundancy, temporal redundancy, and inter-band redundancy. These factors complicate compression dynamics and require efficient management to develop compression strategies tailored to the unique properties of multispectral imagery. In order to achieve lossless compression, this research study investigates an advanced method of hyperspectral image compression that integrates deep recurrent neural networks (RNNs) with multispectral transforms. The purpose of this integration is to take advantage of the complex temporal dependencies and spatial-spectral correlations found in hyperspectral images in order to improve compression performance while maintaining crucial data for further analysis. DWT and PCA are two multispectral transforms that are initially utilized to take advantage of the spatial-spectral redundancies that are naturally present in hyperspectral data. In order to prepare the way for later compression stages, these transforms seek to decorrelate spectral information. To capture complex spatial correlations across the different spectral bands, deep recurrent neural networks which are well-known for their capacity to represent long-range dependencies are introduced as a building block. A synergistic approach to addressing the particular challenges posed by hyperspectral image compression is ensured by the seamless integration of deep RNNs and multispectral transforms. The aim of this work is to create an entire framework that best utilizes the advantages of deep RNNs and multispectral transforms while also achieving lossless compression and faithfully reconstructing the original hyperspectral image. The technique aims to achieve higher ratios without compromising the integrity of important spectral information by adaptively choosing and combining parameters according to the unique features of the hyperspectral data. This research presents a novel method for hyperspectral image compression, adding to the ever-changing field of remote sensing. Enhancing the efficacy and precision in remote sensing applications is possible through the integration of deep recurrent neural networks and multispectral transforms, which presents a promising solution to the problems posed by managing large volumes of hyperspectral data.

This study's key contributions are as follows:

- Development of an advanced compression method for hyperspectral images that uses temporal dependencies and spatial-spectral correlations to seamlessly combine deep recurrent neural networks with multispectral transforms.
- Utilizing Discrete Wavelet Transform (DWT), to optimize the data for further compression stages in order to decorrelate spectral information.
- Enhancing the compression performance by capturing and taking advantage of intricate spatial correlations across the different spectral bands using deep RNN, more especially Long Short-Term Memory (LSTM) networks.
- Integrated spectral and spatial information using deep RNNs and multispectral transforms. This integration seeks to improve compression efficiency by utilizing

the correlation between adjacent pixels and spectral bands.

The structure is organized like the following. Section II explores works that are similar to the current study by exploring into the body of previous literature in the topic. After that, the problem statement is outlined in Section III, along with the particular difficulties that the study attempted to solve. The methodology of the suggested model, including its numerous components and methods, is expounded upon in Section IV. Next, a thorough discussion is started in Section V, which provides a concise summary of the results. Section VI provides a conclusion of the research outcome and considerations for further research.

## II. RELATED WORKS

Li et al. [7] suggested a proposal for remote sensing multispectral image compression using convolution neural networks and multispectral transforms. The benefits of TD, such as Nonnegative Tucker Decomposition, can be used to compress multispectral images. CNN with NTD is the foundation of a low-complexity compression method for multispectral images that was developed. A novel spectrum transform was employed, leveraging CNNs to convert the three-dimensional spectral tensor from a large to small-scale version. The initial and rebuilt three-dimension spectral tensor in self-learning CNNs were minimized in order to produce the optimized spectral tensor for small scale. To increase computation efficiency, the NTD resources only allot the small-scale three-dimension tensor. The result shows that the computation efficiency improved by 49.66% by sacrificing only 0.3369 dB compared to NDT. The drawback is the essential to implement a complex learning network to reduce computational costs.

Cabronero et al. [8] Proposed High-Efficiency Lossless Compression of Spectral Decorrelation. To obtain as many HSI scenes on the ground as possible, data reduction is a crucial tool. Simultaneously, space borne devices' energy and hardware limitations place restrictions on the complexity of workable compression algorithms. In this study, only lossless compression is taken into consideration to prevent any distortion in the analysis of the HSI data. The goal of this work is to determine the optimal trade-off between complexity and compression for high-spatiality HSI compression. The goal of this work is to determine the best possible trade-off between complexity and compression for high-spatiality images (HSI) compression. Results regarding the execution time and compression performance are obtained for a collection of 47 HSI scenes generated by 14 distinct sensors during actual remote sensing missions. The results obtained indicate that the FAPEC algorithm provides the best trade-off, assuming that there is only a finite amount of energy available.

Dua et al. [9] suggested a lossless prediction-based multi-temporal image compression method in this research. It greatly reduces the size of the time-lapse hyperspectral image by eliminating temporal correlations. It uses a linear combination of pixels from previously estimated spectral and temporal bands to predict the target image's pixel value. The RLS filter is used to update the weight matrix that is used in

the prediction. The best number of bands to choose for prediction, the relative strength of each correlation, and the bit-rate efficiency of the method are all shown by the experimental results. According to the findings, adding temporal correlations lowers the bit-rate by 24.07%, and the model optimizes the bits per pixel by 18.15% when compared to the most advanced technique. The disadvantage is that designing a universally applicable solution becomes difficult when automating the entire process and dealing with a variety of datasets and scenarios. Furthermore, the process of creating an automatic model to determine the number of temporal prediction bands might encounter challenges in precisely encapsulating the subtleties of different datasets, which could result in less-than-ideal performance in specific scenarios.

Deng et al. [10] proposed a model, utilizing Generative Neural Networks for Learning-Based Hyperspectral Image Compression. The research presented an alternative method of HSI compression using a GNN, which uses a random latent code to learn the distribution of probability of the actual data. To do this, it's necessary to must define a family of densities and identify the one that minimizes the difference between the actual data distribution and this family. The HSI is then represented by the well-trained neural network, and the complexity of the GNN controls the compression ratio. Additionally, the latent code can be made secret by encrypting it with a random distribution digit embedded in it. To show the GNN potential in resolving compression issues of images in the field of HSI, experimental examples are provided. This work presents a novel neural network-based compression technique and opens up a wide range of new research avenues. Other structures can be added to increase the compression ratio is the major drawback. Additionally, since the neural network can be thought of as a representation of the HSI, the GNN can be used directly for many tasks, including classification, by manipulating its layer to match the classification label.

Makarichev et al. [11] suggested a Quality Controlled Lossy Compression of Three-Channel Remote Sensing data via Discrete Atomic Transform, three-channel RS images are utilized. It is shown how varying and controlling the maximal absolute deviation can affect the quality of images compressed by DAT. Additionally, there is a strict relationship between this parameter and more conventional metrics like PSNR and RMSE, which can be adjusted. Additionally, it is demonstrated that the depths of the various DAT variants vary. A variety of perspectives are used to compare their performances, and transform depth suggestions are provided. The disadvantage is that DAT-based compression cannot be extended to RS data or to other practical tasks like classification of crops, forest cut monitoring, etc.

Grassa et al. [12] proposed a Compression of Hyperspectral Data Using a Fully Convolutional Autoencoder. A new deep convolutional auto encoder architecture-based Spectral Signals Compressor Network. Comprehensive tests were carried out on a variety of multi/hyperspectral and RGB datasets, demonstrating significant gains over baselines and outperforming conventional JPEG family algorithms. The outcomes demonstrate the effectiveness of SSCNet in obtaining better compression ratios and reconstructing spectral

signals, especially showing resilience when dealing with data types larger than 8 bits. Moreover, thorough assessment employing PSNR, SSIM, and MS-SSIM standards consistently demonstrates SSCNet's superiority over current techniques, confirming its mastery of spectral signal compression. The efficacy and accessibility of the framework across RGB, multi spectrum, and hyperspectral sources were proven through extensive experiments on multiple benchmark datasets, which also reported a high compression ratio achieved and an excellent reconstruction.

Changcheng et al. [13] suggested a matrix with an invertible method to eliminate spectral redundancy and improve bit allocation inside the structure. To reduce redundancy, the method combines the DWT's lifting scheme with other strategies like SPIHT coding. The experimental results highlight how well the suggested algorithm performs in lossless compression when compared to well-known techniques. When compared to the previously mentioned algorithms, the results show a significant average compression ratio improvement of roughly 73.6 % respectively, using the JPL Canal test image as a benchmark dataset.

Leo et al. [14] proposed Hyperspectral image compression without losses with recurrent neural networks. The spectral and spatial resolution of hyperspectral images are constantly rising due to the rapid growth of hyperspectral sensor technology, which in turn is causing the scale of hyperspectral data to grow exponentially. Hyperspectral compression with no loss technology is currently at a standstill. At the same time, the emergence of machine learning has given us fresh concepts. Consequently, the application of deep learning to the lossless compression of hyperspectral images is examined in this paper. Given that the DPCM method is inadequate for forecasting spectral band information, a deep (RNN) is used in the proposed C-DPCM-RNN method to enhance the conventional DPCM method and boost the model's capacity for generalization and prediction accuracy. The ultimate experimental outcome demonstrates that C-DPCM-RNN performs better.

Among the difficulties in compressing multispectral images from remote sensing are the need for novel ways to deal with computational complexity, trade-offs between complexity and compression, the need for universality in compression solutions, and the limitations of existing compression techniques in handling a variety of datasets and real-world applications. Multi-temporal image compression challenges include the need to address the limitations of discrete atomic transform (DAT) in order to extend compression methods to other remote sensing data types and useful applications, as well as the development of globally applicable solutions for a variety of datasets and scenarios. New approaches are needed to address these issues and improve the effectiveness and versatility of compression methods in order to improve the state of multispectral image compression.

### III. PROBLEM STATEMENT

Because of the growing amount of hyperspectral imaging data in remote sensing, the previously mentioned literature

identifies common issues with storage, transmission, and computational handling. Traditional compression techniques do not handle the complex temporal dependencies and spatial-spectral correlations found in hyperspectral images. To achieve lossless compression, an advanced compression strategy combining deep recurrent neural networks and multispectral transforms must be established. Some of the challenges are the complex spatial-spectral nature of hyperspectral data, the need for computational efficiency, particularly in real-time applications, the need to record and maintain temporal dependencies, adaptability across diverse datasets, and the need for lossless compression to retain critical information [15]. Resolving these issues is critical for improving remote sensing capabilities and ensuring the preservation of hyperspectral data for applications such as agriculture, disaster relief, and environmental monitoring, among others. The proposed method aims to provide a comprehensive response by optimizing hyperspectral data utilization in ways that are both useful and resource efficient.

### IV. PROPOSED METHODOLOGY FOR EFFECTIVE LOSSLESS HYPER-SPECTRAL IMAGE COMPRESSION

The proposed methodology of this research involves data collection procedure entails obtaining hyper-spectral images, and to improve contrast throughout the spectral bands, histogram equalization is used for image pre-processing. Consistent contrast enhancement is ensured by the adaptability of histogram equalization to multispectral data. This allows for easier compression in the future and balanced information representation. The impact of compression on performance is assessed using pertinent metrics, and parameters are adjusted based on the requirements of the compression model and the characteristics of hyper-spectral data. The pre-processing step incorporates the histogram equalization seamlessly before multispectral transforms are applied and data is fed into a Deep Recurrent Neural Network (DRNN). The process is essential for preserving information fidelity and optimizes compression by emphasizing subtle features. To efficiently capture spatial-frequency information, the compression pipeline incorporates the DWT. The core of DWT is multi-resolution analysis and sub-band coding, which improve compression in conjunction with DRNN and multispectral transforms. The recurrent nature of the DRNN architecture, which propagates historical information through hidden state vectors, is highlighted in detail. Long-short term memory cells are used in the architecture to provide enhanced memory capabilities and selective information retention through gates, helping to overcome issues like gradient vanishing or exploding. Compared to conventional compression techniques, this all-encompassing strategy provides a more holistic representation of the hyper-spectral data and may result in improved compression performance without compromising analytical precision. Furthermore, by employing sophisticated neural network architectures, the model can be made adaptive and learn from the data, which lets it adapt dynamically to various hyper-spectral scene types and maximize compression effectiveness. The block diagram of the proposed methodology is given in the below Fig. 1.

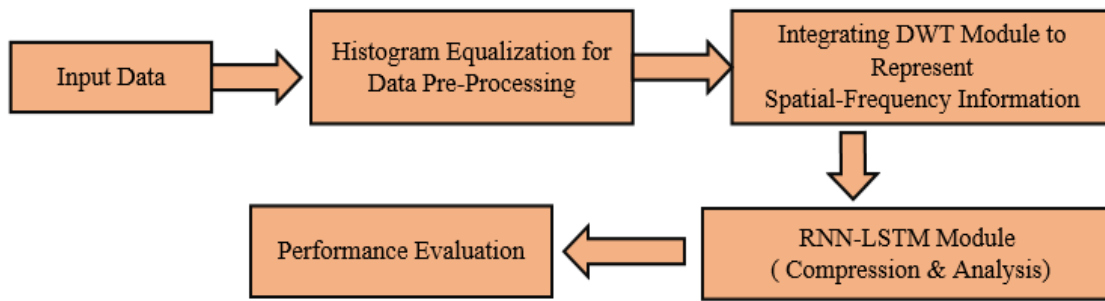


Fig. 1. Overall block diagram of the proposed methodology.

### A. Data Collection

Indian Pines hyperspectral datasets in [16] were utilized in order to validate the efficiency of the proposed method. The Indian Pines dataset is used for hyperspectral image compression. The input data is made up of 145x145 pixel hyperspectral bands covering a single landscape in Indiana, US (Indian Pines data set). The dataset of Indian Pines is gathered by the AVIRIS sensor. The dataset comprises resolution of 20 m and 220 spectral bands spanning from 0.4 to 2.5  $\mu\text{m}$ .

### B. Image Pre-processing using Histogram Equalization

By increasing the contrast of hyper-spectral images, histogram equalization helps to highlight subtle features and may even improve the performance of subsequent compression methods. Consistent contrast enhancement across all spectral bands is ensured by its adaptability to multispectral data, which helps with compression and promotes a more balanced information representation [17]. Histogram equalization supports lossless compression by avoiding information loss brought on by certain characteristics in the original images being difficult to see. Histogram equalization's effect on compression performance should be assessed using pertinent metrics, and parameters should be fine-tuned in accordance with the demands of the compression model and the unique properties of hyper-spectral data. A comprehensive strategy for improving the general quality and efficacy of compression in hyper-spectral imaging is ensured by fully integrating into the pre-processing procedure prior to the application of multispectral transforms and data feeding into the deep recurrent neural network. Histogram Equalization allows for more contrast to be obtained from a smaller localized intensity differential. It seeks to improve the picture's visual attractiveness and ease of analysis. The intensity spreading values of a picture can be seen as arbitrary numbers, ranging from 0 to  $S-1$ . The term "random calculation" can also refer to the accompanying cumulative distribution function. The likelihood that an arbitrary value will be assigned a value that is less than or equal to a given value is defined by this function.

Denote the input image  $f$  as an array of numerical pixels with intensities values within the range of 0 to  $S-1$ , where  $S$  is the intensity probability value. Additionally,  $q$  denotes regularized histogram of the primary image ( $f$ ). Eq. (1) represents the general formula for  $q$  and  $g$ .

$$qn = \frac{\text{number of pixels with intensity } n}{\text{total number of pixels}} \quad n=0, 1, \dots, L-1 \quad (1)$$

Eq. (2) represents the histogram equalization of the image.

$$h_{i,j} = \text{flor}(S-1) \sum_{n=0}^{f_{i,j}} qn \quad (2)$$

The flor ( $\cdot$ ) changed to the closest down integer as a result. This is equivalent to applying the following Eqn. (3) to the values of the densities,  $k$ , of 'f':

$$R(k) = \text{flor}(S-1) \sum_{n=0}^k qn \quad (3)$$

This conversion was inspired by considering the densities for  $f$  and  $h$  as continuous arbitrary values  $T$ ,  $H$  over a time spanning from 0 to  $L-1$ , where  $Z$  is a variable. Eq. (4) represents intensity formula is given below.

$$H = R(T) = (S-1) \int_0^x q(x) dx \quad (4)$$

where,  $q(x)$  is the probability intensity formula for  $g$ .  $R$  is the product of  $T$ 's collective distribution values and product of  $(S-1)$ . It will be easier to suppose that the variable  $U$  is differentiable and invertible. While the function  $U(X)$  denotes  $T$ , which is normally distributed.

### C. Integrating Discrete Wavelet Transform

In 1976, Crochiere introduced sub-band coding for the first time, which laid the groundwork for the discrete wavelet transform [18]. Pyramidal coding, also referred to as multi-resolution analysis, is a method that Burt defined in 1983 and is strikingly similar to sub-band coding [19]. Later, Vetterli and Le Gall eliminated the redundant elements from the pyramidal coding scheme and made some adjustments to the sub-band coding scheme. The system is able to effectively capture and represent the spatial-frequency information present in remote sensing data by adding DWT to the compression pipeline. The combination of DRNN and multispectral transforms improves compression even more, preserving complex features and patterns in hyper-spectral images. This integration opens the door for more precise and efficient downstream analysis in addition to optimizing the transmission and storage of remote sensing data. The combination of these cutting-edge methods is leading the charge in pushing the limits of compression techniques in the context of hyper-spectral imaging, which presents a promising path for improved data management and analysis in remote sensing applications.

The primary signal in DWT is passed through a half-band digital low-pass filter with an impulse response of  $h[n]$ . Eq. (5) illustrates the convolution of the signal.

$$y[n] * h[n] = \sum_{k=-\infty}^{\infty} x[k] \cdot h[n-k] \quad (5)$$

By transferring the signal ( $y[n]$ ) through a half-band low-pass filter, all frequencies higher than half of the primary signal's peak frequency are eliminated. The Nyquist's rule states that half of the samples can be removed. As indicated by Eq. (6), this process involves down sampling (or subsampling) the low-pass filter's output by two.

$$z[n] = \sum_{k=-\infty}^{\infty} h[k] \cdot y[2n - k] \quad (6)$$

This process, which makes up one level of decomposition in DWT, can be mathematically expressed using Eq. (7) and Eq. (8) in which the output of the high and low-pass filters following down sampling is denoted by  $z_{high}[k]$  and  $z_{low}[k]$ .

$$z_{high}[k] = \sum_n y[n] \cdot g[2k - n] \quad (7)$$

$$z_{low}[k] = \sum_n y[n] \cdot h[2k - n] \quad (8)$$

Sub-band coding is the name for this type of decomposition, which doubles frequency resolution and halves time resolution. It can be repeated for additional decomposition by filtering the low-pass filter's output.

The output of DWT is [p3.q3.q2.q1], as shown in Fig. 2. The frequency specifications of the primary signal and its filters are linked to the decomposition levels for DWT. Ultimately, the original signal's DWT is acquired by concatenating all coefficients, commencing from the final decomposition level. Therefore, the DWT coefficients equal the coefficients of the original signal.

#### D. Architecture of Deep Recurrent Neural Networks (RNNs) for Effective Lossless Compression

Using a series of vectors, recurrent architecture can propagate past information to the current unit (i.e., represented by hidden state vectors) through RNN operations. Recurrent neural networks (RNNs) have demonstrated exceptional performance in time-sequence data processing, such as recognizing speech and processing natural languages [20]. The fact that a sample and its predecessors usually have a strong correlation is an important feature of a time sequence. The probability of a particular state in the hidden Markov model, a model that is frequently used in language processing, depends only on its prior state.

Let  $Y = [y_1, y_2, \dots, y_t]$  represent the sequence of data, with  $t$  representing the state label. The data at the first state is represented by  $Y_1$ , and the data at the  $t$  state is represented by  $Y_t$ . One way to formulate the Markov assumption in (9).

$$P(y_t | y_1, \dots, y_{t-1}) = P(y_t | y_{t-1}) \quad (9)$$

where, the conditional probability is expressed by  $P(\cdot)$ . RNN and HMM are comparable in that they both rely on an earlier state for computation of the current state. Unlike traditional ANNs, the RNN processes sequential data in a circular manner, meaning that each data instance in the sequence will receive the same processing, with each state's outcome depending on the state before it. The parameter sharing is also represented by this circular processing. One common technique to limit the number of parameters in a DL scheme is parameter sharing. Nevertheless, assuming

sequential data  $Y = [y_1, y_2, \dots, y_t]$  the hidden state  $r_t$  can be expressed in (10).

$$D_t = f_d(X_{dy}y_t + X_{dd}D_{t-1} + b_t) \quad (10)$$

where,  $X_{dy}$  represents the weight matrix from the source data to the hidden state and  $X_{dd}$ , the current state to the subsequent state. The bias variable is  $b_t$ . The nonlinear function of activation is represented by  $f_d(\cdot)$ , and the hidden state at time step  $t$  is indicated by  $D_t$ . Equation (11) and the output calculation at state  $t$  are very similar.

$$z_t = f_z(X_{dz}D_t + b_z) \quad (11)$$

where,  $X_{dz}$  represents the weight matrix connecting the output and hidden state.  $f_z(\cdot)$  is the nonlinear activation function, and  $b_z$  is the bias.

Since the hidden state ( $D_t$ ) is computed via forward propagation using the previous state as a basis, it can be thought of as the RNN model's memory. Sequential data from earlier states are also taken into account in the interim. Unlike a traditional neural network, some parameters in such forward propagation—such as the three distinct weight matrices  $X_{dd}$ ,  $X_{dy}$ , and  $X_{dz}$ ,—are shared throughout all steps. By reducing the number of trainable parameters, the parameter-sharing scheme improves the efficiency of the entire computation. Fig. 3 depicts the architecture of deep RNN-LSTM is given.

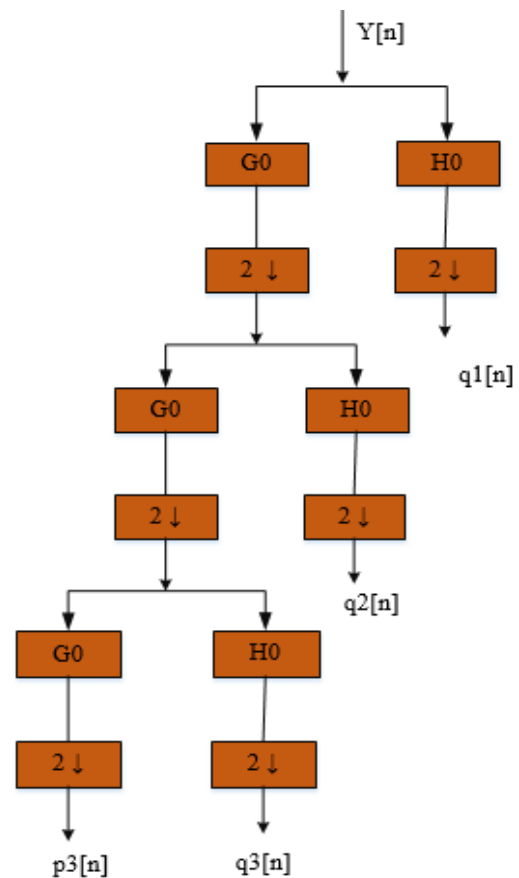


Fig. 2. Architecture of discrete wavelet transforms.

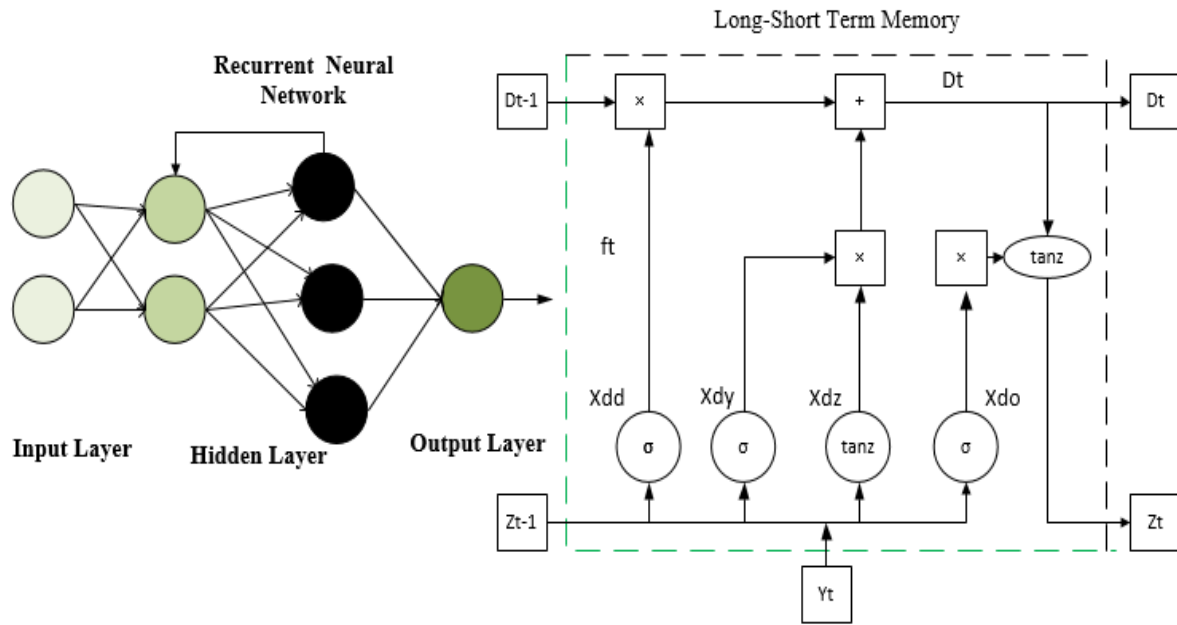


Fig. 3. Deep RNN-LSTM architecture.

LSTM was created using advanced recurrent neuron. Every recurrent neuron in an LSTM can be thought of as a single cell state [21]. LSTM uses the previous state as the input to the current state, just like the traditional RNN. To control the current neuron, the LSTM uses three gates: the forget gate, update gate, and output gate.

An LSTM network has the ability to recall and make connections between data gathered in the past and current. Three gates are coupled with LSTM: an input gate, a forget gate, and an output gate [22]. The input is denoted by  $D_t$  and  $D_{t-1}$ , denotes new and last state respectively, and the current and prior outputs by  $z_t$  and  $z_{t-1}$ .

Fig. 4 depicts the proposed DWT-RNN-LSTM Network model's overall workflow. The DWT-RNN-LSTM Network that has been proposed can efficiently compress hyper-spectral images with greater efficiency, and provide a more trustworthy for the lossless compression of images.

The following forms illustrate the LSTM input gate idea.

$$i_t = \sigma(X_i \cdot [z_{t-1}, y_t] + b_i) \quad (12)$$

$$\tilde{D}_t = \text{tanz}(X_i \cdot [z_{t-1}, y_t] + b_i) \quad (13)$$

$$D_t = f_t D_{t-1} + i_t \tilde{D}_t \quad (14)$$

where, Eq. (12) determines which piece of data should be added by passing  $z_{t-1}$  and  $y_t$  through a sigmoid layer. When  $z_{t-1}$  and  $y_t$  have travelled through the tanz layer, Eq. (13) is

then used to get new information. In Eq. (14), the long-term storage data  $D_{t-1}$  into  $D_t$  and the present moment information,  $\tilde{D}_t$ , are merged.  $X_i$  denotes a sigmoid output, while  $\tilde{D}_t$  stands for tanz output. Here,  $b_t$  stands for the LSTM input gate bias while  $X_i$  stands for weight matrices. The LSTM's forget gate then enables the dot product and sigmoid layer to selectively pass information. With a certain probability, the choice of whether to delete relevant data from an earlier cell is carried out. Eq. (15) is used to determine whether or not to retain relevant information from a preceding cell with a particular chance.  $X_f$  stands for weight matrix,  $b_f$  for offset, and  $\sigma$  for sigmoid function.

$$f_t = \sigma(X_f \cdot [z_{t-1}, y_t] + b_f) \quad (15)$$

The output gate of the LSTM ascertains the necessary states for the subsequent Eq. (16) and Eq. (17) states provided by the  $z_{t-1}$  and  $y_t$  inputs. After obtaining the final output, the state decision vectors that send fresh data,  $D_t$ , via the tanz layer are multiply by it.

$$P_t = \sigma(X_o \cdot [z_{t-1}, y_t] + b_o) \quad (16)$$

$$z_t = P_t \text{tanz}(D_t) \quad (17)$$

where, the weighted matrices  $X_o$  and the bias  $b_o$ , respectively.

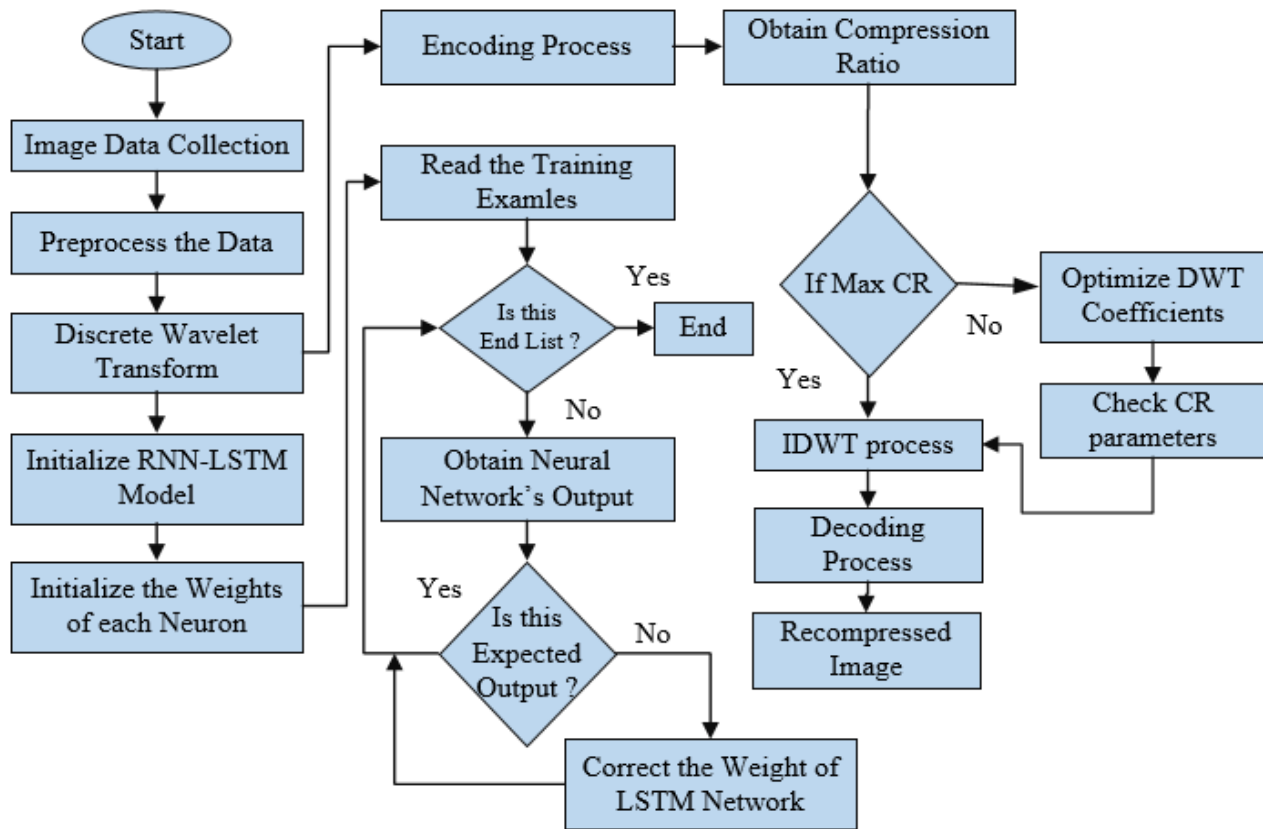


Fig. 4. Overall flow chart of DWT-RNN-LSTM method.

## V. RESULTS

The outcomes of the proposed methodology demonstrates how well it works to achieve optimal compression and consistent contrast enhancement for better data analysis in remote sensing applications. In order to ensure balanced information representation, histogram equalization is used as a pre-processing step, demonstrating its adaptability to multispectral data. By combining DWT with LSTM cells and deep recurrent neural network (DRNN), problems such as gradient vanishing or exploding are avoided and information fidelity is preserved while historical data is retained selectively. The methodology's success in capturing subtle features and managing hyper-spectral data efficiently is confirmed by the assessment of the impact of compression using pertinent metrics. The talk focuses on the potential for further developments, such as the investigation of optimization methods, incorporation of more machine learning algorithms, creation of models for adaptive compression, and expansion of applications to different remote sensing fields. On the Anaconda platform, the programming language of choice was Python. The following metric was used to assess the model's efficiency. The influence of compression on performance is carefully examined using appropriate metrics, and model parameters are changed depending on the compression model's unique requirements and the intrinsic properties of hyper-spectral data. This complete approach assures that the suggested technology not only accomplishes effective compression but also maintains information

integrity, which is critical for remote sensing applications. Finally, the model's benefit is its ability to smoothly incorporate histogram equalization, multispectral transforms, DRNNs, and DWT, resulting in a comprehensive solution for advanced lossless compression in hyper-spectral image.

### A. Performance Evaluation

Metrics for performance evaluation, like PSNR and MSE are essential for determining the quality of compressed or reconstructed images. Even though these metrics provide quantitative insights, subjective assessments are frequently added to obtain a complete picture quality assessment. A comparison is made between the suggested model and the performance of LSMA based compression, STW-WDR, and DPCM.

1) *PSNR*: PSNR for simple terms is a metric frequently used to assess the effectiveness with which an image has been compressed. When comparing the quality of a reconstructed or compressed hyperspectral image to the original, PSNR can be used to assess hyperspectral images, which are images taken in multiple bands across the electromagnetic spectrum.

The following Eq. (18) is used to determine the PSNR:

$$PSNR = 10 \cdot \log_{10} \left( \frac{MAX^2}{MSE} \right) \quad (18)$$

- The maximum pixel value that an image can have been referred to as MAX (255 for 8-bit images, for example).



- The average of the squared pixel-wise differences between the original and compressed images is termed as the Mean Squared Error, or MSE.

Since a higher PSNR value suggests less distortion or error in the compressed image, it typically denotes higher image quality. A higher PSNR is preferred in lossless compression since the objective is to reach high compression ratios without sacrificing the quality of the original image.

2) *Mean Square Error*: MSE is a statistic frequently used to express the average squared differences between matching pixels in two different images. MSE is frequently used in image processing and compression to assess how well a reconstructed or compressed image compares to the original.

The following Eq. (19) is the formula for mean squared error:

$$MSE = \frac{1}{n \times m} \sum_{p=1}^n \sum_{q=1}^m (I(p, q) - L(p, q))^2 \quad (19)$$

- The intensity of the corresponding pixel in the original image is represented as I (p, q).
- In a compressed or reconstructed image, L (p, q) denotes the intensity of the corresponding pixel.

The squared difference between each pair of corresponding pixels is used to calculate the mean square error (MSE). This squared difference is then added up and divided by the total number of pixels (n × m). Better image fidelity is implied by a lower MSE value, which shows less variation between the original and reconstructed images. MSE, however, may not always correspond with human visual perception and does not directly account for perceptual differences. Because of this, when assessing image quality, it is frequently used in conjunction with other metrics and subjective evaluations.

The performance metrics of several image compression techniques, such as LSMA-based compression, STW-WDR, DPCM, and the suggested DWT-RNN, are compared in the Table I. The suggested DWT-RNN approach outperforms all other techniques in terms of PSNR, attaining a noticeably higher value of 45 dB. Additionally, it exhibits better Mean Squared Error (MSE) performance than the other methods, with the lowest value of 7.50%, indicating improved compression efficiency and image quality. These other methods include LSMA based compression, STW-WDR, and DPCM.

TABLE I. THE SUGGESTED METHOD'S PERFORMANCE METRICS ARE COMPARED TO THOSE OF EXISTING METHODS

Methods	PSNR (dB)	MSE (%)
LSMA based Compression [23]	33	20.57
STW-WDR [24]	35	18.02
DPCM [25]	30	17.09
Proposed DWT-RNN	45	7.50

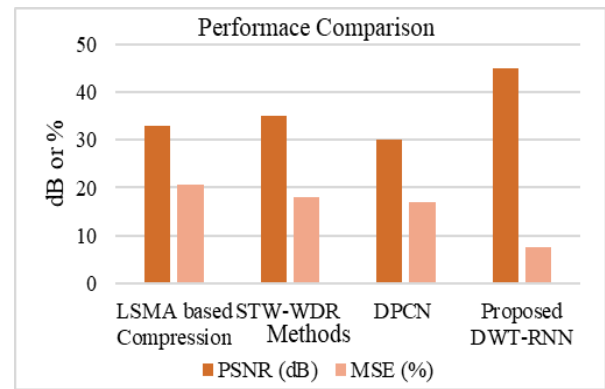


Fig. 5. Performance comparison with the existing methods.

Fig. 5 shows a graphical representation of the suggested performance metrics in comparison to the current methods. The proposed DWT-RNN-LSTM method demonstrates the highest PSNR Value when compared with existing methods.

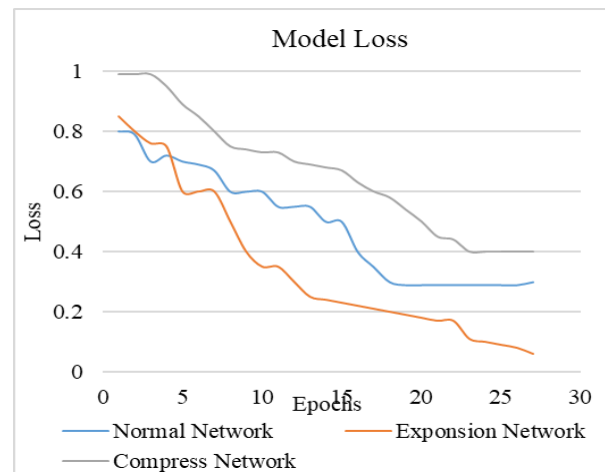


Fig. 6. Proposed DWT-RNN-LSTM method's loss is illustrated graphically.

The loss values against number of epochs are shown in Fig. 6. It shows the overall loss from the proposed DWT-RNN-LSTM Method's Loss is illustrated graphically.

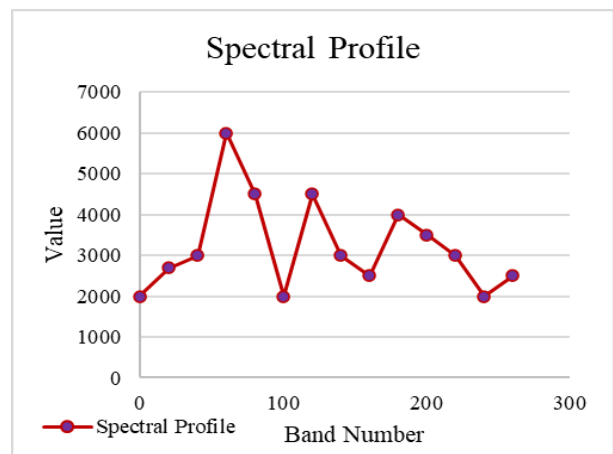


Fig. 7. Proposed DWT-RNN-LSTM method's spectral profile is illustrated graphically.

Fig. 7 depicts the graphical illustration of Spectral profile of the proposed model. The spectral profile is a critical component in advanced remote sensing image compression method because it allows for lossless compression in hyper-spectral imaging. The distribution of electromagnetic energy across different wavelengths, which captures the distinct signature of materials present in a scene, is referred to as the spectral profile. Optimizing compression efficiency requires combining deep recurrent neural networks (RNNs) with multispectral transforms.

TABLE II. PSNR OF DWT-RNN-LSTM METHOD IN EACH COMPRESSED RATION

Compression Ratio	PSNR (dB)
1	45
2	44
3	42
4	40
5	38
6	33
7	30
8	25

Table II represents the PSNR of DWT-RNN-LSTM method in each compressed RATION and it exhibits an effective lossless compression output.

Fig. 8 depicts the graphical illustration of PSNR of the proposed model. Higher PSNR values indicate better original information preservation. It provides a numerical measure of image fidelity by quantifying the ratio of the signal strength of maximum values to the noise introduced during compression.

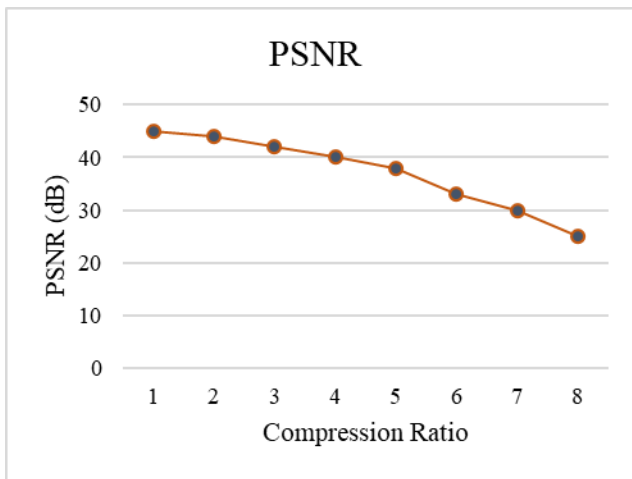


Fig. 8. Proposed DWT-RNN-LSTM method's PSNR is illustrated graphically.

### B. Discussion

The proposed approach to hyperspectral image compression shows notable improvements in attaining ideal compression and contrast enhancement for remote sensing applications by integrating DWT with LSTM cells and deep recurrent neural network. The approach's flexibility in

handling multispectral data is demonstrated by the pre-processing step of histogram equalization, which guarantees balanced information representation. When DWT is combined with LSTM and DRNN, problems like gradient vanishing or exploding are successfully resolved, maintaining information fidelity and keeping some historical data. PSNR and MSE, are three performance evaluation metrics that show how much better the suggested DWT-RNN approach is than the state-of-the-art techniques like LSMA-based compression [23], STW-WDR [24], and DPCM [25]. In comparison to other methods, the higher PSNR value of 45 dB and lower MSE of 7.50% show better compression efficiency and superior image quality.

A graphic confirmation of the methodology's effectiveness can be seen. A performance comparison with current approaches is mentioned clearly, where the higher PSNR value of the suggested DWT-RNN is highlighted. The loss values are plotted against the number of epochs is shown graphically, which shows how stable and convergent the model was during training. The spectral profile of the suggested model highlights the significance of combining multispectral transforms and deep recurrent neural networks for the best compression in hyperspectral imaging. Lastly, Figure 8 shows the PSNR of the suggested model graphically, highlighting how well it can retain original data. Together with the quantitative metrics, these visual aids offer a thorough evaluation of the effectiveness of the suggested methodology for advanced hyperspectral image compression in remote sensing applications.

### VI. CONCLUSION AND FUTURE SCOPE

In conclusion, this comprehensive and inventive hyper-spectral image compression methodology employs DRNN with long-short term memory cells, multispectral transforms, and histogram equalization for contrast enhancement. Problems like gradient vanishing and explosion are solved by incorporating the DWT, and spatial-frequency information capture is improved. The compression parameters are adjusted adaptively based on the needs of the model and the properties of the hyper-spectral data to ensure efficiency. Deep recurrent neural networks and multispectral transformations may limit real-time processing capabilities or necessitate high-performance computing infrastructure due to their probable requirement for large computational resources during both the training and compression phases. Future research directions include looking into more complex optimization strategies, incorporating more machine learning algorithms, developing adaptive compression models, investigating hardware acceleration, and expanding applications to different remote sensing domains, and designing intuitive user interfaces and visualization tools. This methodology establishes a solid foundation for future research into the compression of hyper-spectral images for various remote sensing applications.

### REFERENCES

[1] R. Dusselaar and M. Paul, "Hyperspectral image compression approaches: opportunities, challenges, and future directions: discussion," *JOSA A*, vol. 34, no. 12, pp. 2170–2180, Dec. 2017, doi: 10.1364/JOSAA.34.002170.

- [2] D. Heller Pearlshien and E. Ben-Dor, "Effect of Organic Matter Content on the Spectral Signature of Iron Oxides across the VIS–NIR Spectral Region in Artificial Mixtures: An Example from a Red Soil from Israel," *Remote Sens.*, vol. 12, no. 12, Art. no. 12, Jan. 2020, doi: 10.3390/rs12121960.
- [3] S. Agrawal, S. Debnath, S. Sagnika, S. Bilgaiyan, and S. Gupta, "Hyperspectral Image Compression using Modified Convolutional Autoencoder," 2022.
- [4] Y. Dua, R. S. Singh, K. Parwani, S. Lunagariya, and V. Kumar, "Convolution Neural Network based lossy compression of hyperspectral images," *Signal Process. Image Commun.*, vol. 95, p. 116255, Jul. 2021, doi: 10.1016/j.image.2021.116255.
- [5] R. Qureshi, M. Uzair, K. Khurshid, and H. Yan, "Hyperspectral document image processing: Applications, challenges and future prospects," *Pattern Recognit.*, vol. 90, pp. 12–22, Jun. 2019, doi: 10.1016/j.patcog.2019.01.026.
- [6] G. Morales, J. W. Sheppard, R. D. Logan, and J. A. Shaw, "Hyperspectral Dimensionality Reduction Based on Inter-Band Redundancy Analysis and Greedy Spectral Selection," *Remote Sens.*, vol. 13, no. 18, Art. no. 18, Jan. 2021, doi: 10.3390/rs13183649.
- [7] J. Li and Z. Liu, "Multispectral Transforms Using Convolution Neural Networks for Remote Sensing Multispectral Image Compression," *Remote Sens.*, vol. 11, no. 7, p. 759, Mar. 2019, doi: 10.3390/rs11070759.
- [8] M. Hernández-Cabronero, J. Portell, I. Blanes, and J. Serra-Sagristà, "High-Performance Lossless Compression of Hyperspectral Remote Sensing Scenes Based on Spectral Decorrelation," *Remote Sens.*, vol. 12, no. 18, p. 2955, Sep. 2020, doi: 10.3390/rs12182955.
- [9] Y. Dua, R. S. Singh, and V. Kumar, "Compression of multi-temporal hyperspectral images based on RLS filter," *Vis. Comput.*, vol. 38, no. 1, pp. 65–75, Jan. 2022, doi: 10.1007/s00371-020-02000-6.
- [10] C. Deng, Y. Cen, and L. Zhang, "Learning-Based Hyperspectral Imagery Compression through Generative Neural Networks," *Remote Sens.*, vol. 12, no. 21, p. 3657, Nov. 2020, doi: 10.3390/rs12213657.
- [11] V. Makarichev, I. Vasilyeva, V. Lukin, B. Vozel, A. Shelestov, and N. Kussul, "Discrete Atomic Transform-Based Lossy Compression of Three-Channel Remote Sensing Images with Quality Control," *Remote Sens.*, vol. 14, no. 1, p. 125, Dec. 2021, doi: 10.3390/rs14010125.
- [12] R. La Grassa, C. Re, G. Cremonese, and I. Gallo, "Hyperspectral Data Compression Using Fully Convolutional Autoencoder," *Remote Sens.*, vol. 14, no. 10, p. 2472, May 2022, doi: 10.3390/rs14102472.
- [13] C. Li, D. Chen, C. Xie, Y. Gao, and J. Liu, "Research on Lossless Compression Coding Algorithm of N-Band Parametric Spectral Integer Reversible Transformation Combined With the Lifting Scheme for Hyperspectral Images," *IEEE Access*, vol. 10, pp. 88632–88643, 2022, doi: 10.1109/ACCESS.2022.3199737.
- [14] J. Luo, J. Wu, S. Zhao, L. Wang, and T. Xu, "Lossless compression for hyperspectral image using deep recurrent neural networks," *Int. J. Mach. Learn. Cybern.*, vol. 10, no. 10, pp. 2619–2629, Oct. 2019, doi: 10.1007/s13042-019-00937-2.
- [15] H. Shen, Z. Jiang, and W. D. Pan, "Efficient Lossless Compression of Multitemporal Hyperspectral Image Data," *J. Imaging*, vol. 4, no. 12, Art. no. 12, Dec. 2018, doi: 10.3390/jimaging4120142.
- [16] "Indian Pines - V7 Open Datasets." Accessed: Nov. 22, 2023. [Online]. Available: <https://www.v7labs.com/open-datasets/indian-pines>.
- [17] C. S. Yadav et al., "Multi-Class Pixel Certainty Active Learning Model for Classification of Land Cover Classes Using Hyperspectral Imagery," *Electronics*, vol. 11, no. 17, p. 2799, Sep. 2022, doi: 10.3390/electronics11172799.
- [18] M. B. I. Reaz, M. Akter, and F. Mohd-Yasin, "Image Compression System for Mobile Communication: Advancement in the Recent Years," *J. Circuits Syst. Comput.*, vol. 15, no. 05, pp. 777–815, Oct. 2006, doi: 10.1142/S0218126606003301.
- [19] M. Z. Baghbidi, "Improvement of Anomaly Detection Algorithms in Hyperspectral Images Using Discrete Wavelet Transform," *Signal Image Process. Int. J.*, vol. 2, no. 4, pp. 13–25, Dec. 2011, doi: 10.5121/sipij.2011.2402.
- [20] A. Ma, A. Filippi, Z. Wang, and Z. Yin, "Hyperspectral Image Classification Using Similarity Measurements-Based Deep Recurrent Neural Networks," *Remote Sens.*, vol. 11, no. 2, p. 194, Jan. 2019, doi: 10.3390/rs11020194.
- [21] R. C. Staudemeyer and E. R. Morris, "Understanding LSTM -- a tutorial into Long Short-Term Memory Recurrent Neural Networks." arXiv, Sep. 12, 2019. Accessed: Nov. 21, 2023. [Online]. Available: <http://arxiv.org/abs/1909.09586>.
- [22] Md. Z. Islam, Md. M. Islam, and A. Asraf, "A combined deep CNN-LSTM network for the detection of novel coronavirus (COVID-19) using X-ray images," *Inform. Med. Unlocked*, vol. 20, p. 100412, 2020, doi: 10.1016/j.imu.2020.100412.
- [23] G. Zhang, S. Mei, M. Ma, Y. Feng, and Q. Du, "Spectral Variability Augmented Sparse Unmixing of Hyperspectral Images," *IEEE Trans. Geosci. Remote Sens.*, vol. 60, pp. 1–13, 2022, doi: 10.1109/TGRS.2022.3169228.
- [24] R. Nagendran and A. Vasuki, "Hyperspectral image compression using hybrid transform with different wavelet-based transform coding," *Int. J. Wavelets Multiresolution Inf. Process.*, vol. 18, no. 01, p. 1941008, Jan. 2020, doi: 10.1142/S021969131941008X.
- [25] J. Li, J. Wu, and G. Jeon, "GPU Acceleration of Clustered DPCM for Lossless Compression of Hyperspectral Images," *IEEE Trans. Ind. Inform.*, vol. 16, no. 5, pp. 2906–2916, May 2020, doi: 10.1109/TII.2019.2893437.